EXPENDITURE

The funds expended for the period from July 2003 to the end of February 2004 are set out in the table below:

Expense Category	**Amount Approved**	**Amount Spent**
Salary, scientific personnel	$50,000	$21,000*
Salary, technical personnel	$61,000	$30,000
Consumables	$120,628	$99,000
Overheads	$30,500	$27,000
Totals	$262,128	$177,000

* There have been major savings in the professional staff salaries this year because the person carrying out the CIR aspect of the project is now a full time Ph.D. student with a scholarship provided by the University of Sydney. Major aspects of the ketosteroid CIR work form part of his research.

Proposal for Year 2

The original proposal was for a two-year program with the major expenditure occurring in the first year. In the second year the EPO glycoform project will be completed within the first four months and will involve statistical of the data and preparation of a scientific paper summarising the work and its major findings. The CIR measurements will continue but the methodology used will change. The ketosteroid analysis will be essentially complete and the analysis of steroidal diols will begin. The ketosteroid analysis is much simpler than the diol analysis but in some cases of doping with endogenous steroids the diol methodology is the only one that will give a definitive result. We had hoped to develop a simple method for diol extraction and purification prior to GC-CIRMS analysis such as we have done for the ketosteroids, but it appears at this stage that an extensive cleanup using HPLC will be required. Because of this the number of samples that can be analysed using the resources available will need to reduced from the 1000 stated in the original budget. On current estimates the number of samples that can be analysed will be approximately 500. The samples to be analysed will be chosen from the EPO2000 samples using the data already obtained from the ketosteroid analyses with a view to optimising the subject diversity and hence the statistical significance of the data obtained.

The major objectives for Year 2 are –

- Complete the statistical analysis of the EPO glycoform results and prepare a publication on the results of this study.
- Complete the statistical analysis of the ketosteroid GC-CIRMS measurements and prepare a publication on the results of this study.
- Begin the analysis of steroidal diols using GC-CIRMS with the view to having a statistically significant dataset completed by mid 2005.

References

Aguilera, R., Chapman, T.E., Catlin D.H., (2000) A rapid screening assay for measuring urinary androsterone and etiocholanolone delta 13C values by gas chromatography/combustion/isotope ratio mass spectrometry. Rapid Communications in Mass Spectrometry, 14:2294-2299.

Cawley A., Rogerson J., Rahman K., Trout G., Kazlauskas R. (2004) Preliminary results on the carbon isotope ratios of ketonic steroids in urine samples collected from different countries. Recent Advances in Doping Analysis (11). W. Schanzer, H. Geyer, A. Gotzmann, and U. Mareck-Engelke (eds), Sport und Buch Strauss, Cologne, 2004, 183-193.

Egrie, J.C., Browne J.K., (2001), Development and characterisation of novel erythropoiesis stimulating protein (NESP). Brit J. Cancer 84(Suppl 1):3-10.

Howe C. (2003) Personal communication from F. Lasne of LNDD Paris

Lasne F, Martin L., Crepin N., de Ceaurriz J. (2002) Detection of isoelectric profiles of erythropoietin in urine: differentiation of natural and administered recombinant hormones, Anal. Biochem., 311, 119-126.

Morrison, D.J., Dodson, B., Slater, C., Preston, T. (2000) Carbon 13 natural abundance in the British diet: implications for 13C breath tests. Rapid Communications in Mass Spectrometry, 14:1321-1324.

Ohta, M., Kawasaki, N., Hyuga, S., Hyuga, M., Hayakawa, T., (2001) Selective glycopeptide mapping of erythropoietin by on-line high-performance liquid chromatography-electrospray ionization mass spectrometry.

Shackleton, C.H., Phillips, A., Chang, T., Li, Y., (1997), Confirming testosterone administration by isotope ratio mass spectrometric analysis of urinary androsatanediols. Steroids, 62:379-387.

ELSEVIER

Available online at www.sciencedirect.com
SCIENCE DIRECT•

Journal of Chromatography A, 1020 (2003) 273–282

JOURNAL OF
CHROMATOGRAPHY A

www.elsevier.com/locate/chroma

Analysis of quantization error in high-precision continuous-flow isotope ratio mass spectrometry

Gavin L. Sacks, Christopher J. Wolyniak, J. Thomas Brenna*

Savage Hall, Division of Nutritional Sciences, Cornell University, Ithaca, NY 14853, USA

Received 10 June 2003; received in revised form 8 August 2003; accepted 12 August 2003

Abstract

High-precision isotope ratio mass spectrometry (IRMS) systems are equipped with digitizers that deliver effective maximum digitization depths of 16 to 24 bits; however, there are no analyses of the proper board depth required to retain high precision in continuous-flow techniques. We report an experimental and theoretical evaluation of quantization error in continuous-flow IRMS (CF-IRMS). CO_2 samples (100 pmol–30 nmol) were injected into a gas chromatography combustion IRMS system (GC–CIRMS). The analog signal was digitized by high precision, 24-bit ADC boards at 10 Hz, and was post-processed to simulate 12, 14, and 16-bit data sets. $\delta^{13}C_{pdb}$ values were calculated for all data sets by the conventional "summation" method or by curve-fitting the chromatographic peaks to the exponentially modified Gaussian (EMG) function. Benchmarks of S.D.($\delta^{13}C_{pdb}$) = 0.3, 0.6, and 1.0‰ were considered to assess precision. In the presence of significant quantization noise, curve-fitting required several-fold less CO_2 than the summation method to reach a given benchmark. We derived an equation to describe the theoretical limitations of precision for the summation method as a function of CO_2 admitted to the source and the step size of the boards. Theory was in close agreement with the observed lower limit of precision for the simulated 16-bit data set. Curve-fitting achieved a precision of S.D. <0.3‰ for injections 20-fold smaller than summation for CO_2 samples collected on an IRMS with 16-bit resolution. By mitigating the impact of quantization noise, curve-fitting expands the dynamic range within a single run to include lower analyte levels, and effectively reduces the need for high pumping capacities and high precision ADC boards.

Keywords: Isotope ratio mass spectrometry; Mass spectrometry; Quantization error; Carbon dioxide

1. Introduction

Isotope ratio mass spectrometry (IRMS) coupled to a gas chromatography–combustion interface (GC–C) can routinely measure relative differences in $^{13}C/^{12}C$ isotope ratios to a precision of few parts per million for samples containing 10 ng of sample or less [1,2]. GC–CIRMS data consists of three concurrent chromatographic traces ($^{44}CO_2$, $^{45}CO_2$, $^{46}CO_2$) from three detectors operated in parallel. Achieving high precision requires careful and consistent definition of background levels and peak integration for all three traces. Most commonly, peak areas are integrated by the "summation" method. The start and end of a peak are detected, and the background is described as a square or trapezoidal area beneath the peak. Raw data are summed over the length of the peak, and the background area is subtracted. Ricci et al. [3] described two

---

* Corresponding author. Tel.: +1-607-255-9128; fax: +1-607-255-1033.
E-mail address: jtb4@cornell.edu (J.T. Brenna).

0021-9673/$ – see front matter © 2003 Elsevier B.V. All rights reserved.
doi:10.1016/j.chroma.2003.08.022

general methods for determining the background using summation; the "individual summation" method, in which the background is defined by connecting low points on either side of the peak, and the "dynamic summation" method, in which low points are connected throughout the chromatogram regardless of the location of peaks.

All IRMS instruments use digitizers to convert analog signal from Faraday cups to digital data, which must be processed to yield isotope ratios. The precision of a digitizer is expressed in terms of bits, where an N-bit board has 2^N steps over a given range. As an example, a 16-bit board has ~65 000 steps; if the board has a range of 0–10 V, then the step size of the board is ~0.15 mV. The rounding of a continuous signal to discrete steps introduces noise, which is referred to as quantization error or "bit noise". This effect is shown graphically in Fig. 1, where simulated Gaussian peaks of 24, 16, 14, and 12-bit resolution are presented. At high resolution (24 bits), no quantization noise is noticeable, and the peak appears as a smooth trace. As the resolution decreases, steps become obvious, and the shape of the peak deteriorates. The quality of data reduction in continuous-flow IRMS must depend at least in part on the digitizer depth because the intensity level established for peak start and stop depends on this parameter. As depth decreases, the intensity of the background is, in general, less well represented by the intensity levels of the peak's start and stop points. There are no analyses available that establish the relationship between isotope ratio precision and digitization depth.

The effect of digitization depth on precision and accuracy is inextricably linked to data reduction algorithms. The reproducibility of the summation background correction depends in part on the two points that anchor the background line under the peak; imprecision in the measurement of either point multiplies through the entire length of the background segment connecting the points. In the presence of a simple linear background, a background line is easily drawn between any two points on either side of the peak, as shown in Fig. 2a. Chemical noise due to column bleed or contaminant peaks may cause inaccuracy in defining the background, but such noise is usually correlated in all three traces. This covariance may mitigate the effects of chemical noise on the calculated isotope ratio. However, in the case of quantization error, as shown in Fig. 2b, the magnitude and direction of error is uncorrelated among the three traces, and this then poses a special case. Our previous work has shown that peak integration by curve-fitting improves precision and accuracy in cases of low signal-to-noise [4] and overlapping peaks [5]. Background correction

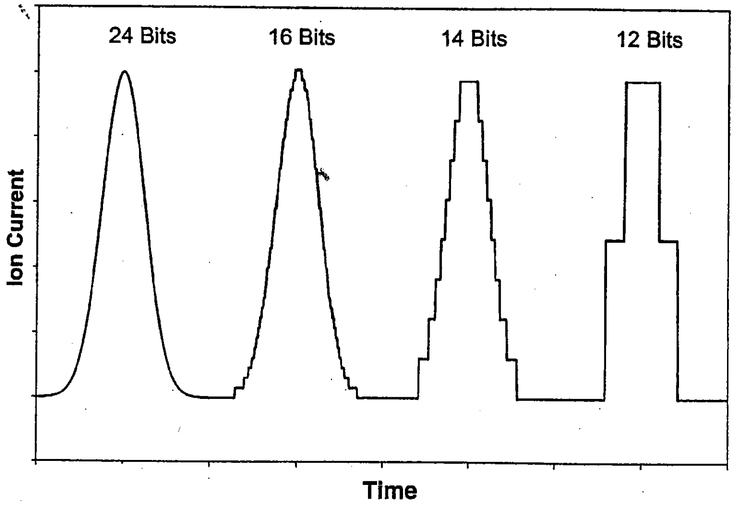

Fig. 1. A simulation of a Gaussian signal collected by ADCs of various resolutions (24, 16, 14, and 12 bits) and quantization errors. At 24-bit resolution, quantization error is not visible, and the peak appears as a smooth trace. At 16 bits, bit noise is evident primarily at the base of the peak. At 12-bit resolution, the signal is barely recognizable as a Gaussian shape.

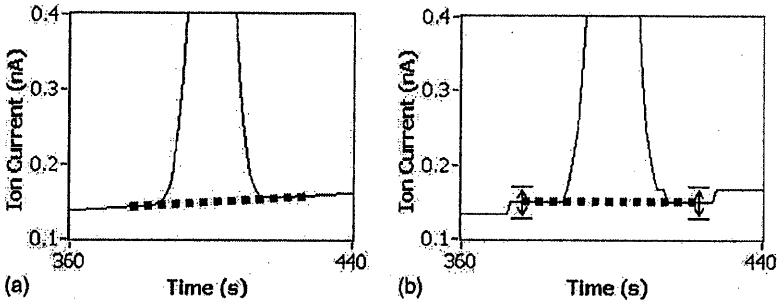

Fig. 2. Simulated chromatographic peaks in the presence of a linearly rising background (a) without and (b) with quantization error. In the presence of quantization error, the true background may fall anywhere within the arrows. Without quantization error background is easily and accurately achieved by connecting points on either side of the peak.

in curve-fitting is not constrained to the actual values represented by the discrete digitization levels, and we hypothesized that it may not be as sensitive to quantization error as summation.

Quantization error is typically not dominant in GC–CIRMS when high precision IRMS data acquisition systems use sufficiently deep digitization boards and signals are sufficiently strong. Noise from other sources, such as chemical noise, is greater than the step size of the digitizers. However, quantization error may become important in two specific situations: (a) in data reduction of minor peaks in a chromatogram where there are fewer steps between baseline and peak top, and (b) when low precision digitizers are used, as is common in low cost IRMS instruments designed primarily for measurements of high abundance samples, such as CO_2 in breath tests. In addition, these systems usually have lower pumping capacity, which limits the flow rate that the IRMS source accepts. The lower inlet flow rates result in smaller signals for equivalent analyte abundance via higher split ratios, making quantization error more prominent. In this report, we evaluate quantization error theoretically and experimentally to determine the limiting the precision achieved by the conventional summation algorithm and by curve-fitting.

2. Experimental

2.1. Instrumentation

A Varian 3400 GC system was coupled via a combustion furnace to one of two gas IRMS instruments: (a) a FinniganMAT 252 (FMAT252) run in high linearity mode, or (b) an Analytical Precision Products 2003 (APP2003). Both IRMS systems were operated with a source pressure of 1×10^{-6} Torr and had an absolute sensitivity of ~5000 mol/ion (1 Torr = 133.322 Pa). The GC–C system is described in detail elsewhere [6]. Briefly, the effluent from the capillary column (60 m × 0.32 mm, 0.25 μm, BPX70; SGE, Austin, TX, USA) is directed to a combustion furnace filled with CuO and held at 850 °C, and dried in a Nafion water trap before admittance to the IRMS system through an open split. Since CO_2 gas was injected as a sample, the combustion step was not necessary, but was retained in the system to increase the verisimilitude to real GC–CIRMS operating conditions. The FMAT252 has differential pumping and a higher overall pumping capacity, while the APP2003 has only a single turbopump. As a result, the FMAT252 can tolerate higher inlet flow rates. The open split of the FMAT 252 accepted 0.2 ml/min (split ratio = 8.4:1), and the open split of the APP2003 accepted 0.07 ml/min (split ratio = 24:1).

CO_2 (Airgas East, 99.9%) injections were performed by hand consecutively. The split ratio and the injection size were varied to yield between 100 pmol and 30 nmol on column. Four or five replicates were performed for each injection size. The moles of CO_2 in each injection were approximated by assuming ideal gas conditions.

Data was collected on the FMAT 252 using SAXICAB [7], a laboratory-built LabVIEW-based [8] data acquisition system employing National Instruments (Austin, TX, USA) 435× digitizers yielding

24 bits operating at 10 Hz. Data were collected on the APP2003 using the vendor-supplied 16-bit, 10 Hz data acquisition system. Both systems simultaneously monitored the $m/z = 44$, 45, and 46 cups with >99% duty cycle.

2.2. Data processing

Before data reduction, data collected from the FMAT 252 at 24 bits was rounded on all three traces to simulate 16-, 14-, and 12-bit data sets. The head amplifiers have a maximum signal of 10 V (33 nA for $m/z = 44$), so the step size, Δ, for a given board depth was calculated as:

$$\Delta = \frac{10\,\mathrm{V}}{2^{\mathrm{bits}}} \qquad (1)$$

We created simulated data sets by rounding data points to the nearest step:

$$\mathrm{data(quantized)} = \mathrm{round}\left[\frac{\mathrm{data(raw)}}{\Delta}\right]\Delta \qquad (2)$$

where, the *round* function rounds the input to the nearest whole number.

The 16-bit data from the APP2003 was used without modification. All data sets were processed using SAXICAB by either the individual summation method or by curve-fitting. The individual summation method used by SAXICAB was adapted from Ricci et al. [3]. Starts and stops of peaks were determined with a slope sensitivity of 0.3 nA/s. The lowest point 2 s before and 2 s after the peak limits were located, and a straight line was drawn between the two points to define the background. In the curve-fitting algorithm, the traces were fit to exponentially modified Gaussian (EMG) functions using the Levenberg–Marquardt algorithm. Mathematical details of the EMG function can be found elsewhere [9].

High-precision isotope ratios are expressed in the delta (‰) notation:

$$\delta^{13}\mathrm{C}_{\mathrm{pdb}} = \frac{{}^{13}R_{\mathrm{spl}} - {}^{13}R_{\mathrm{pdb}}}{{}^{13}R_{\mathrm{pdb}}} \times 1000 \qquad (3)$$

where ${}^{13}R_x$ is the ratio of ^{13}C to ^{12}C, SPL refers to the sample, and PDB refers to the international standard, PeeDee Belemnite, where ${}^{13}R_{\mathrm{pdb}} = 0.0112372$. In our work, δ^{13}C of the CO_2 injections were calculated using pulses of standard CO_2 gas that had been indirectly calibrated to the PDB reference. The contribution of ^{17}O to the ${}^{45}CO_2$ signal was taken into account by the method of Santrock et al. [10]. No outliers were excluded from the reported data.

3. Results and discussion

3.1. Observed effects of quantization error

Fifteen CO_2 injection amounts were used to produce peak areas on the FMAT 252 that varied over 2.5 orders of magnitude. The peaks showed excellent symmetry and narrow peak widths, with a full width at half maximum of <3 s. The mean reproducibility of the area for each injection size, as measured by the area of the $m/z = 44$ signal, was R.S.D. = 13%. Plots of $\delta^{13}\mathrm{C}_{\mathrm{pdb}}$ versus injection size, shown in Fig. 3, are displayed for both the curve-fitting (a) and individual summation (b) methods. The plots are similar in appearance to those presented by others [11] investigating the performance of GC–CIRMS at low signal levels.

In agreement with our previous work [4], we observe modest improvement of precision at low signal levels using the curve-fitting method. Using the summation method, precision deteriorates (S.D. > 1.0‰) for injection sizes less than 400 pmol on column (~50 pmol to the IRMS). Curve-fitting improves this limit to 175 pmol on column (~20 pmol to the IRMS). The integration methods performed comparably and acceptably at large injection sizes. For on-column injections of at least 6.8 nmol (~800 pmol to the IRMS), the individual summation method had a precision of S.D.($\delta^{13}\mathrm{C}_{\mathrm{pdb}}$) = 0.1‰. The curve-fitting method gave slightly worse precision for large injections, S.D.($\delta^{13}\mathrm{C}_{\mathrm{pdb}}$) = 0.2‰. It is not obvious why the summation method out-performs the curve-fitting method for very large sample sizes. One possibility is that the precision of the curve-fitting method is limited by differences between the shape of the model EMG function and the shape of real, chromatographic peaks. In this case, increasing the injection size past a certain point would not improve the fit, even though S/N is increasing. Using a different function to describe the peaks may further improve results.

To assess the tolerance of the two integration methods to quantization noise, we evaluated simulated

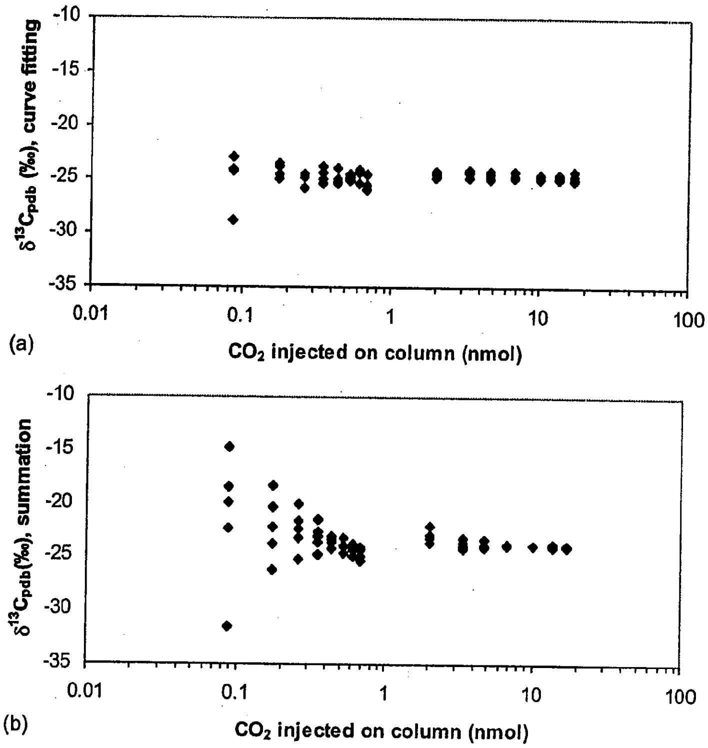

Fig. 3. $\delta^{13}C_{pdb}$ vs. CO_2 injected on column for (a) curve-fitting and (b) individual summation algorithms. Data was collected using a homebuilt system at 24 bits from FMAT252.

12, 14, and 16-bit raw data sets generated from the raw 24-bit FMAT252 data, and processed both by curve-fitting and summation. The accuracy of successive injections was very good, even in the presence of bit noise. For each method, the mean $\delta^{13}C$ for any two injection sizes did not differ significantly. Plots of S.D.($\delta^{13}C_{pdb}$) versus CO_2 injected on column at all bit resolutions are shown in Fig. 4. Each plot appears to extend asymptotically along the x- and y-axes, and we can evaluate the dependence of precision on quantization error visually; poor performance is indicated by the asymptotic plot moving up and away from the axes. At 24-bit resolution, plots of the summation and curve-fitting methods nearly overlap, except at very small injection amounts, indicating that performance is similar. With increasing quantization error, the minimum amount of CO_2 necessary to reach a given level of precision increases rapidly for the summation method. Curve-fitting is more forgiving; precision from 14- and 16-bit data is comparable to the 24-bit data. The plot for 12-bit resolution shows some loss of precision, but does not fare as badly as the summation method.

To evaluate the methods objectively, we defined S.D.($\delta^{13}C_{pdb}$) = 0.3, 0.6 and 1.0‰ as benchmarks for high precision. The data were least-squares fitted to a power function, of the form:

$$\text{S.D.} = A[CO_2]^B \tag{4}$$

where $[CO_2]$ is the moles of CO_2 injected on column, S.D. is the observed precision, and A and B are constants. The power function was chosen for empirical reasons, because it modeled the observed data acceptably, and the fitted curves can then be compared. The best-fit lines for both the summation (dashed) and curve-fitting (solid) methods are shown in Fig. 4. From the best-fit equations, we calculated the amount of CO_2 injected on-column necessary to achieve the 0.3, 0.6, and 1.0‰ benchmarks (Fig. 5). With least quantization error (24-bit resolution), the

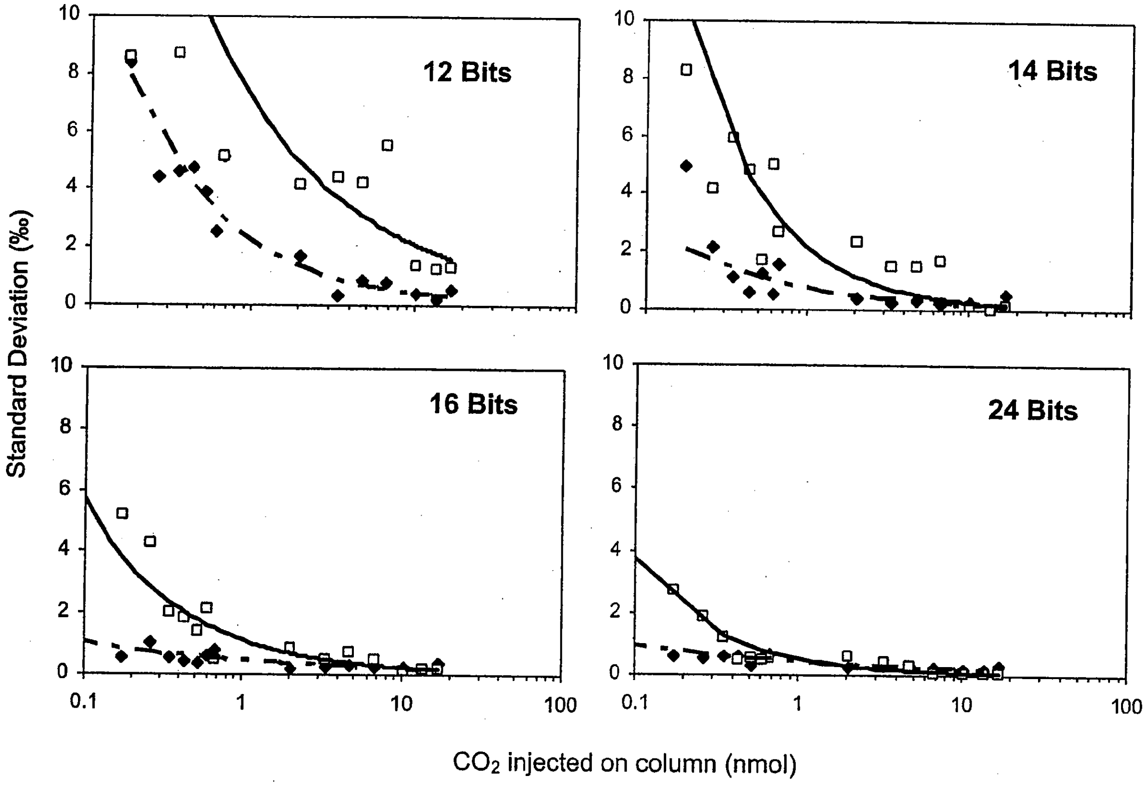

Fig. 4. S.D.($\delta^{13}C_{pdb}$) vs. CO_2 injected on column at 12-, 14-, 16-, and 24-bit resolutions, calculated by summation (□) or curve-fitting (◆) algorithms. Each point represents four or five replicates. The data for each method and each resolution was fit to a power equation (general form: S.D. $=A[CO_2]^B$, and the best-fit lines are drawn for both methods (solid line: summation; dashed line: curve-fitting).

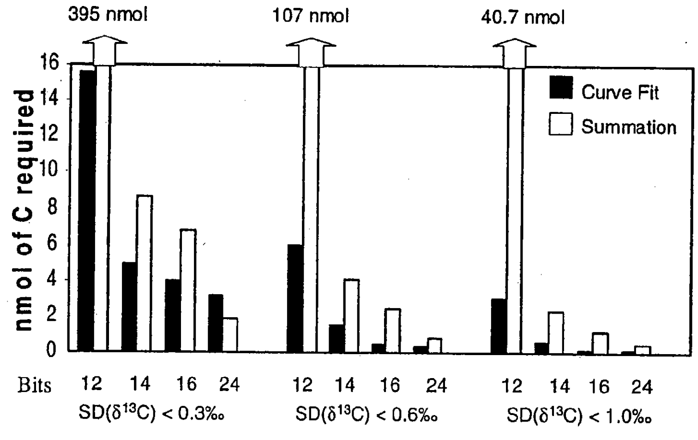

Fig. 5. Carbon required on-column, in nanomoles, to reach a specified level of precision for a given ADC board resolution. Results are shown for data reduced by curve-fitting and summation algorithms.

summation method requires slightly less CO_2 than the curve-fitting method at the 0.3‰ benchmark (1.86 nmol versus 3.19 nmol). At 16-bit resolution, the summation method requires 6.83 nmol, an increase of 267%, compared to a 25% increase for curve-fitting over the same interval. To reach the 0.6‰ benchmark at 16 bits, summation requires an increase of 224% (from 0.77 to 2.50 nmol), compared to 33% for curve-fitting. At 12-bit resolution, the amount of CO_2 on column necessary to achieve S.D. = 0.6‰ by summation is 107 nmol, which far exceeds the capacity of the GC column. Curve-fitting requires only 6 nmol to reach S.D. = 0.6‰ at 12-bit resolution. As was discussed previously, curve-fitting is superior to summation at the 1.0‰ benchmark, even in the absence of quantization noise. At 24 bits, curve-fitting requires 80 pmol to achieve S.D. = 1.0‰, five-fold less than summation; a similar level of improvement in precision is seen at 14- and 16-bit resolution.

To summarize, in the absence of quantization noise, similar amounts of CO_2 are necessary to achieve precision of 0.3–0.6‰ for both integration methods. The summation method requires a dramatic increase in the injection size to maintain this level of precision in the presence of quantization noise, while the curve-fitting method is relatively unaffected. At a lower standard of precision (S.D. = 1.0‰), curve-fitting is superior regardless of the magnitude of quantization error.

3.2. Theoretical limits of quantization error on precision

In IRMS, the signal is recorded as a voltage proportional to the ion current, and can be reported in amperes or in volts. If the signal is reported in volts, the area of the $m/z = 44$ signal, A_{44}, is related to the moles of $^{44}CO_2$ that enters the IRMS, $[^{44}CO_2]$, by the equation:

$$A_{44} = [^{44}\mathrm{CO_2}]\frac{N_\mathrm{a}e}{E}R_\Omega \qquad (5)$$

where N_a is Avogadro's number, e is the fundamental charge, E is the absolute sensitivity of the IRMS in molecules/ion, and R_Ω is the feedback resistance of the amplifier.

In the summation method, the background is defined by drawing a line between two background points, (t_1, y_1) and (t_2, y_2); the background area, A, is the trapezoidal region between this line and the time axis. We can calculate this area by the equation:

$$A(\text{background}) = \tfrac{1}{2}W(y_1 + y_2),\quad \text{where } W = t_2 - t_1 \qquad (6)$$

Quantization noise is uniformly distributed over an interval and the error for a single measurement is:

$$\sigma_y = \frac{\Delta}{\sqrt{12}} \qquad (7)$$

where Δ is the minimum step size of the acquisition boards. A full derivation of this can be found in Haykin's text on digital communication [12]. Assuming that quantization error at y_1 and y_2 is uncorrelated, we can use standard techniques for propagation of errors to determine the total quantization error in measuring the background area, σ_A:

$$\sigma_A = \frac{W\Delta}{2\sqrt{6}} \qquad (8)$$

It has been noted that evaluating the effect of chemical noise on precision of isotope ratios is difficult, because this noise is usually highly correlated between the major and minor traces [11]. Unlike chemical noise, quantization noise on each trace should be uncorrelated. This greatly simplifies calculation of the propagation of errors for the relation of the observed isotope ratio, $^{45}R_\mathrm{obs}$, to the actual isotope ratio, $^{45}R_\mathrm{act}$:

$$^{45}R_\mathrm{obs} = \frac{A_{45} \pm \sigma_{45}}{A_{44} \pm \sigma_{44}} = {}^{45}R_\mathrm{act} \pm \sigma_\mathrm{obs} \qquad (9)$$

where

$$\sigma_\mathrm{obs} = {}^{45}R_\mathrm{act}\sqrt{\left(\frac{\sigma_{45}}{A_{45}}\right)^2 + \left(\frac{\sigma_{44}}{A_{44}}\right)^2} \qquad (10)$$

The standard error can be rearranged and expressed in terms of parts per thousand:

$$\sigma_\mathrm{ppt} = 1000 \times \frac{\sigma_\mathrm{obs}}{^{45}R_\mathrm{act}} = 1000 \times \sqrt{\left(\frac{\sigma_{45}}{A_{45}}\right)^2 + \left(\frac{\sigma_{44}}{A_{44}}\right)^2} \qquad (11)$$

At natural abundance, $A_{45} \sim 0.011A_{44}$. Assuming the feedback resistance is 100× larger for the 45 cup than for the 44 cup, $\Delta_{45} = 0.01\Delta_{44}$. Combining this and Eqs. (5), (8) and (11), we arrive at:

$$\sigma_\mathrm{ppt} = \frac{276W\Delta_{44}E}{[^{44}\mathrm{CO_2}]N_\mathrm{a}eR_\Omega} \qquad (12)$$